

Multi-objective topology optimisation for acoustic porous materials using gradient-based, gradient-free and hybrid strategies

Vivek T. Ramamoorthy,^{1, a)} Ender Özcan,^{1, b)} Andrew J. Parkes,^{1, c)}
Luc Jaouen,^{2, d)} and François-Xavier Bécot^{2, e)}

¹Computational Optimisation and Learning Lab, School of Computer Science, University of Nottingham, NG8 1BB, United Kingdom

²Matelys-Research Lab, 7 Rue des Maraîchers, Vaulx-en-Velin, 69120, France

When designing passive sound-attenuation structures, one of the challenging problems that arise is optimally distributing acoustic porous materials within a design region so as to maximise sound absorption while minimising material usage. To identify efficient optimisation strategies for this multi-objective problem, we compare several gradient, non-gradient and hybrid strategies. For gradient approaches, the solid-isotropic-material-with-penalisation method (SIMP) and a novel gradient-based constructive heuristic (CHg) are considered. For gradient-free approaches, hill climbing with a weighted-sum scalarisation (HC) and a non-dominated sorting genetic algorithm II (NSGA-II) are considered. Optimisation trials are conducted on seven benchmark problems involving rectangular design domains in impedance tubes subject to normal-incidence sound loads. The results indicate that while gradient methods can provide quick convergence with high-quality solutions, often gradient-free strategies are able to find improvements in specific regions of the Pareto front. Two novel hybrid approaches (HA1 and HA2) are proposed combining a gradient method (CHg) for initiation and a non-gradient method (respectively HC and NSGA-II) for local improvements. A novel and effective Pareto-slope-based weighted-sum hill climbing is introduced for local improvement. Results reveal that for a given computational budget, the hybrid methods can consistently outperform the parent gradient or non-gradient methods.

©2023 Acoustical Society of America. [<http://dx.doi.org/XXX>]

[Editor: XYZ]

¹ **Keywords:** Acoustic porous materials; topology optimisation; sound absorption; multi-objective optimisation;

4 I. INTRODUCTION

⁵ Acoustic porous materials such as foams or fibrous materials are widely used for passive noise control in automotive, aerospace and construction industries. While these materials generally exhibit sound absorption across wide frequency bands, their low-frequency absorption performance is poor since the lengths of the absorber typically

¹² needed are higher for longer wavelengths¹. To alleviate this problem, one can modify the absorber shape or introduce macro-scale air cavities² to alter the dynamic properties creating favourable resonances that improve absorption while also reducing the material usage. However, optimising the size, shape and placement of these air cavities or other solid scattering materials³ is essentially a topology optimisation problem⁴, which is challenging to solve.

²² Topology optimisation is the concept of simultaneously optimising both the topology (number of holes in a structure) and the shape (geometry and dimensions of these holes) of mechanical structures so as to maximise the load-bearing capacity with minimal material usage. It is a concept first introduced by Bendsoe and Kikuchi^{5,6} in the 1990s and has remarkable potential benefits in terms of reduced weight and costs. In the last two decades, topology optimisation techniques have been extended to automatic generation of optimised acoustic shape designs in various applica-

^{a)} vivek.thaminniramamoorthy@nottingham.ac.uk, ORCID:0000-0002-1147-6579

^{b)} ender.ozcan@nottingham.ac.uk, ORCID: 0000-0003-0276-1391

^{c)} andrew.parkes@nottingham.ac.uk, ORCID: 0000-0002-8847-1856

^{d)} luc.jaouen@matelys.com, ORCID: 0000-0002-3141-800X

^{e)} fxb@matelys.com, ORCID: 0000-0001-6892-8436

tions, such as horns⁷, room sound treatments⁸, anechoic chamber foams^{2,9}, mufflers^{10–13}, sound barriers^{14–17}, and car internal cavities¹⁸ to name a few. Although topology optimisation is inherently a multi-objective problem i.e., simultaneously maximising performance and minimising weight, it has been common to treat it as a single-objective problem i.e., maximising the performance while using a constraint on the weight. Given that one of the main benefits is the potential weight savings, it is of interest to treat it as a multi-objective problem and obtain multiple trade-off designs simultaneously. The acoustic designers can then choose from the set of Pareto optimal or trade-off solutions for manufacture.

While new and improved optimisation strategies are being published for particular applications, there is a need for comparison studies which would facilitate engineers to choose effective strategies for their use case. Performing such comparisons is challenging since many optimisation paradigms exist to solve topology optimisation problems that vary in solution representation (discrete or continuous), gradient usage, memory (single point or population-based), move operators, acceptance strategies etc. To ensure a fair comparison, each algorithm needs to be applied in the best or most reasonable settings tuned to the problem. In this article, a few selected approaches that are popular and likely to be used by other researchers are tested and compared. The list of approaches chosen are:

- Solid isotropic material with penalisation (SIMP)
- Constructive heuristic with gradient (CHg)
- Hill climbing with weighted-sum scalarisation (HC)
- Non-dominated sorting genetic algorithm-II (NSGA-II)

SIMP is the most commonly-used approach for structural topology optimisation^{19–21}. A key attribute of this approach is the relaxation of the discrete problem into a continuous problem by allowing intermediate materials and using a power-law interpolation scheme. Using continuous relaxation allows the possibility of computing the gradients quickly using adjoint-like methods, which can make the optimisation quite effective, notwithstanding certain drawbacks such as getting stuck at local optima or the presence of intermediate materials in the final solution. Its effectiveness and ease of implementation²², have made it the most popular approach for topology optimisation. At this point, it is worth noting some previous efforts toward extending SIMP for multi-objective topology optimisation. Suresh et al.²³ extended the 99-line MATLAB code to a 199-line code for Pareto-optimal compliance minimisation, and also studied the effect of restarts vs hot starts. Hence, in this

article, two variants SIMPsweep and SIMPrestart are considered. Mirzendehtdel et al.²⁴ proposed a multi-objective algorithm for multi-material compliance minimisation removing the mass constraint and treating it as an objective. While the multi-objective consideration is prevalent, it constitutes a small fraction of the publications, and comparison studies are rare.

Constructive heuristics are a class of optimisation algorithms that start from empty solutions and build them step by step using specific move operations to reach a complete solution. An example of a constructive heuristic for topology optimisation is the (bi-directional) evolutionary structural optimisation methods (ESO/BESO) introduced by Xie and Steven^{25,26}. For compliance minimisation, ESO starts from a completely solid-filled design domain and incrementally removes material from low-stress regions. For acoustic material topology optimisation, Ramamoorthy et al.⁹ introduced two constructive heuristics: CH1, where the material is added incrementally to an empty domain in places of highest absorption increase; and CH2, where the material is incrementally removed from a filled domain from places where the decrease in absorption is minimal. These heuristics performed among the top strategies in the study. One of the drawbacks of CH1 and CH2 is that computing the numerical absorption increments is expensive, and this can be overcome by making use of the gradients. Adopting this, a simple gradient-based constructive heuristic (CHg) is proposed in the current study.

Hill climbing is a single objective optimisation technique that starts with an initial solution and modifies it iteratively while accepting improving changes. A row-wise hill climbing approach was found to perform among the best strategies for acoustic material absorption maximisation⁹. A common strategy to solve multi-objective problems is to combine the objectives into a scalar value in a process known as scalarisation²⁷, and to apply a single objective algorithm. A simple way to scalarise is to use the weighted sum of the objectives. By varying the weights, the relative importance of each objective can be controlled. In this study, hill climbing is used in conjunction with a weighted-sum scalarisation technique (HC) as a candidate for multi-objective topology optimisation.

The non-dominated sorting genetic algorithm-II (NSGA-II) introduced by Deb et al.²⁸ is a well-known multi-objective evolutionary algorithm. A notable attribute of NSGA-II is the use of a fast non-dominated sorting procedure in combination with a crowding-distance operator that allows finding multiple points in the Pareto front simultaneously, as opposed to having to run multiple trials of a single objective algorithm in combination with a scalarisation technique. The effectiveness of NSGA-II and its variants has made it the most

153 popular multi-objective approach for solving combinatorial optimisation problems²⁹.

154
155 In addition to the above strategies, two hybrid approaches (HA1 and HA2) are proposed involving
156 a gradient method for initialisation and a non-gradient method for local improvement. The aim
157 is to find whether hybrid approaches are beneficial. The results will provide perspectives on each
158 method, and guide algorithm selection.
159
160

161
162 The article is organised as follows. In section II, the overall methodology including problem
163 description, optimisation formulation, modelling method, and details of the experimental design
164 is provided. In section III, a comparison of gradient algorithms —SIMP sweep, SIMP restart
165 and CHg is provided. In section IV, a comparison of gradient-free algorithms HC, and NSGA-II
166 are provided. Along with gradient-free algorithms, a random search procedure is also compared.
167 In section V, two hybrid approaches HA1 and HA2 are described and compared with their parent
168 approaches. Finally, in section VI, a summary of the findings and some general guidelines to design
169 algorithms are provided.
170
171
172
173
174
175
176

177 II. METHODOLOGY

178 A. Problem formulation

179 Consider the problem of optimally filling a rectangular design domain with a given porous material
180 such that the sound absorption is maximised while using minimal material. The design domain
181 can be assumed to be backed by rigid walls with normal-incidence acoustic source placed as shown
182 in Figure 1(a). Sound absorption is the ratio of energy absorbed to the total input sound energy. If
183 no porous material is placed in the design domain, there would not be any absorption. Typically as
184 more porous material is filled in the design domain, the absorption would increase, but this is not
185 always the case. There are instances when removing material would improve absorption⁹. Depending
186 on the distribution of porous material and air in the design domain, sound absorption will be
187 determined at different frequencies of the acoustic source. Thus, this is a classic bi-objective
188 optimisation problem with trade-off solutions.
189
190
191
192
193
194
195
196
197

198 While there are many ways to formulate the topology optimisation problem, one of the classical
199 ways is to use a fixed discretisation of the system and optimising the material assigned to each
200 finite element. The shape and topology can be represented by a vector χ with zeros and ones
201 corresponding to the absence or presence of porous material in each element respectively, as shown
202 in Figure 1(b). This is sometimes referred to as a bit-matrix representation³⁰. At this point,
203 it is also worth acknowledging other formulations such as moving morphable components³¹, level-set
204 method^{32,33} etc. The objective considered is to
205
206
207
208
209
210

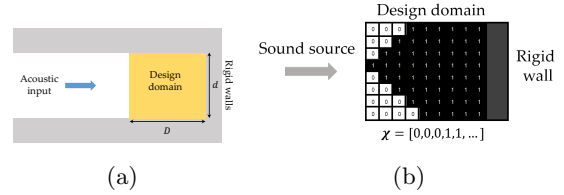


Figure 1. (color online) (a) Schematic of an acoustic system with the design domain. (b) Binary representation of a sample shape. 0 refers to air and 1 refers to porous material.

211 find the optimal discrete assignments of either air
212 or a given poroelastic material to each finite element that simultaneously maximises the normal
213 sound absorption and minimises the volume fraction of the porous material. Mathematically, this
214 formulation can be written as:
215
216

Simultaneously,

$$\max_{\chi} \quad \bar{\alpha}(\chi) = \frac{1}{n_f} \sum_{i=1}^{n_f} \alpha(\chi, f_i) \quad (1)$$

$$\min_{\chi} \quad V_f(\chi) = \frac{1}{n_e} \sum_{i=1}^{n_e} \chi_i \quad (2)$$

$$\chi \in \{0, 1\}^{n_e}$$

$$\bar{\alpha} \in [0, 1]$$

$$V_f \in [0, 1]$$

217 The first objective $\bar{\alpha} \in [0, 1]$ is the sound absorption averaged across the target frequencies
218 (f_1, f_2, \dots, f_{n_f}), and the second objective V_f is the porous volume fraction. Absorption $\bar{\alpha}$ is averaged
219 over a number of target frequencies n_f , and porous material volume fraction V_f is averaged over the
220 number of elements n_e in the design domain.
221
222
223

224 B. Computing the objectives

225 Computing the volume fraction V_f for a given shape χ is quite straightforward from Equation 2,
226 whereas computing absorption $\bar{\alpha}$ is computationally expensive requiring solving a system of linear
227 equations. The procedure followed to compute absorption is the same as outlined in Ramamoorthy
228 et al.⁹. The acoustic system is modelled using the unified Biot-Helmholtz model introduced
229 by Lee et al.², which considers air as a poroelastic material with negligible solid-part behaviour.
230 In the unified model, air is considered to have $\chi_{air} = 0.001$ to avoid numerical issues when solving
231 the system. Lee et al. also verified the validity of such modelling for poroelastic materials with
232 mixed formulations³⁴.
233
234
235
236
237
238
239

240 The most expensive part of computing $\bar{\alpha}$ is finding the solution $\{\mathbf{X}\}$ to a system of linear
241 equations $[\tilde{\mathbf{S}}(\chi, f)]\{\mathbf{X}\} = \{\tilde{\mathbf{F}}\}$, where the system
242

matrix $[\tilde{\mathbf{S}}(\boldsymbol{\chi}, f)]$ is a square symmetric complex-valued matrix with dimensions of the order of the number of finite elements in the design domain, and $\{\tilde{\mathbf{F}}\}$ is the dynamic forcing vector of the same dimension. The system matrix $[\tilde{\mathbf{S}}(\boldsymbol{\chi}, f)]$ is populated with material properties of air or porous material at specific submatrices depending on the shape $\boldsymbol{\chi}$. When considering continuous relaxation, for the intermediate materials i.e. $\chi_i \in (0, 1]$, the material properties are interpolated using a power-law i.e. any material property, say ψ_i is given by $\psi_{air} + \chi_i^p(\psi_{por} - \psi_{air})$, where ψ_{por} and ψ_{air} are the properties of the porous material and air respectively.

Since evaluating absorption $\bar{\alpha}$ is the computational bottleneck and other algorithmic processes take a relatively insignificant amount of time, this is an expensive optimisation problem, and hence it is reasonable to use the number of absorption evaluations to benchmark the performance of algorithms.

Computing the gradient of sound absorption with respect to the design variables takes approximately two more instances of solving the system of linear equations, making it twice as expensive as computing absorption:

$$\text{timeToCompute}\left(\frac{\partial \bar{\alpha}}{\partial \boldsymbol{\chi}}\right) = 2 \times \text{timeToCompute}(\bar{\alpha}) \quad (3)$$

Such a quick computation of the gradient is achieved using a fictitious load vector pre-multiplication, as explained in Lee et al.¹². Thus, computing both absorption and the gradient is 3 times as expensive as computing just absorption. Therefore, the gradient methods will be given one-third the fitness evaluation budget.

C. Benchmark problem instances

To compare the optimisation approaches, seven benchmark problem instances previously introduced in Ramamoorthy et al.⁹ are adopted. The only difference here is that a modification has been made in the mesh size in problem instance 3 in order to improve the model accuracy. For completeness, the details of the problem instances are provided in Table I. All the problem instances have a rectangular design domain but with varying discretisation, the porous material filled, frequency range of interest, and dimensions. Table II provides the poroelastic material properties for the materials used in the problem instances. While the problem instance 1 uses the same material as Lee et al.² with a high tortuosity, the third problem instance uses a fictitious material with high airflow-resistivity, and all other problem instances use melamine.

Table I. Benchmark problems (see section II C)

Problem instance	Mesh size nelx × nely	Length D (m)	Height d (m)	f_{min} Hz	f_{step} Hz	f_{max} Hz	Material ID (see Tab. II)
1	10 × 10	0.135	0.054	100	100	1500	(1)
2	15 × 10	0.045	0.1	100	100	1500	(2)
3	50 × 20	0.1	0.1	50	50	500	(3)
4	10 × 10	0.02	0.1	100	100	1500	(2)
5	10 × 10	0.02	0.1	2000	1000	5000	(2)
6	50 × 20	0.135	0.054	100	100	1500	(2)
7	10 × 5	0.135	0.054	500	500	500	(2)

Table II. Materials used in the benchmark problems and their properties (see Table I).

Material parameters	Material-1	Material-2	Material-3
Material:	LKKK ²	Melamine	High-resistivity foam
Acoustic model:	JCAL ³⁵⁻³⁷	JCAL	JCAL
ϕ	0.9	0.99	0.8
Λ' (μm)	449	196	100
Λ (μm)	225	98	10
σ ($\text{N}\cdot\text{s}\cdot\text{m}^{-4}$)	25000	10000	300000
α_∞	7.8	1.01	3
k'_0	4.75e-09	4.75e-09	4.75e-09
ρ ($\text{kg}\cdot\text{m}^{-3}$)	31.08	8	80
E (Pa)	800000	160000	30000
ν	0.4	0.44	0.44
η	0.265	0.1	0.01

D. Experimental design

Table III provides a quick summary of the optimisation approaches used in this study along with a short description and pseudocode of each approach. More detailed descriptions of each algorithm are provided in the following sections. Reasonable effort has been made to use each algorithm in its recommended or best settings from parameter tuning and has been used in the standard way unless otherwise stated.

All the strategies were given the same arbitrarily-chosen computational budget of 4096 equivalent gradient-free fitness evaluations. Gradient algorithms are assigned $4096/3 \approx 1365$ fitness evaluations, and the non-gradient methods are allowed 4096 fitness evaluations. For the hybrid algorithms, 25% of the computational effort was allotted for gradient-based search and 75% for non-gradient search i.e., $25\% \times 4096/3$ gradient-included and $75\% \times 4096$ gradient-free fitness evaluations.

It should be noted, that in some trials on some problem instances, the resulting SIMP solutions had intermediate materials. In such scenarios, only the non-dominated solutions were discretised by a round-off filter and the fitnesses were recomputed. This is done so that all solutions compared in this

Table III. Optimisation approaches and their settings

Algorithm	Description and pseudocode	Deterministic or stochastic	Trials	Fitness evaluation budget per trial
Gradient-based approaches				
SIMPrestart	Solid isotropic material with penalisation (SIMP) restarted with different volume fraction constraints fixed for a trial: A gradient-based strategy with optimality criteria move-update; following ³⁸ . Initialised trial with an empty design domain; Restarted with a new \bar{V}_f until budget is used up.	Stochastic: multiple restarts within trial	1 (multiple restarts)	1365 (with gradient)
SIMP sweep	SIMP with adaptive volume fraction constraint: Initialised with an empty design domain; Volume fraction constraint \bar{V}_f updated after each fitness evaluation reached 1 as budget approaches.	Deterministic	1	1365 (with gradient)
CHg	Gradient-based constructive heuristic: Start from an empty solution; Add porous material in steps of ‘ m ’ elements where the gradient is highest, until all elements are porous	Deterministic	1	$\min(N/m, 1365)$ (with gradient)
Non-gradient approaches				
HC	Hill climbing: Use a weighted-sum scalarisation technique to combine the two objectives into a single fitness value. Apply first improvement hill climbing starting from a random discrete solution. Move order is like in a raster-scan.	Stochastic, since initial solution is random	15	4096 (non-gradient)
NSGA-II	Non-dominated sorting genetic algorithm -II ²⁸ : Use a bit representation, tournament selection based on crowding distance and rank, uniform crossover, bit-wise mutation probability of $1/N$.	Stochastic	15	4096 (non-gradient)
RAND	Random search algorithm: Picked a desired volume fraction uniformly $\in [0, 1]$; Use this as the probability of porous material at each element and synthesise a solution. Repeat budget number of times.	Stochastic	15	4096 (non-gradient)
Hybrid approaches				
HA1	Hybrid approach 1: Run CHg using 25% of the budget, and run hill climbing for 75% of the budget starting from a selected solution with scalarisation weight such that the combined objective isoline at the solution point in objective space is tangential to the Pareto front.	Deterministic but depends on the point picked for hill climbing	15	4096 (equivalent non-gradient)
HA2	Hybrid approach 2: Run CHg using 25% of the budget, and run NSGA-II for 75% of the budget starting from an initial population from equispaced points in the CHg Pareto front.	Stochastic	15	4096 (equivalent non-gradient)

study are from the discrete space to facilitate a fair comparison.

To quantify and compare the non-dominated solution set produced by each algorithm, a hypervolume metric will be used. The hypervolume value corresponding to a given set of trade-off solutions is the scalar value equal to the union of volumes in the objective space dominated by each

solution over and above the objective values of a given reference solution. An illustration is shown in Figure 2. For the bi-objective problem under study, the hypervolume would simply be the area of the objective space that is dominated by the Pareto set obtained from the algorithms from a reference point. The reference point chosen is $(\bar{\alpha}, \bar{V}_f) = (0, 1)$. Larger the hypervolume, the bet-

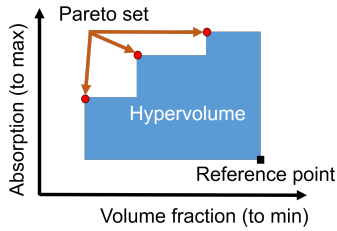


Figure 2. (color online) An illustration of the hypervolume metric.

338 ter the multiobjective performance can be consid-
 340 ered to be.

341 III. GRADIENT APPROACHES

342 A. Solid-isotropic-material-with-penalisation(SIMP)

343 Solid-isotropic-material-with-penalisation
 344 (SIMP) is a popular strategy for structural
 345 topology optimisation where the main idea is to
 346 consider a continuous relaxation of the material
 347 choices by using a power-law interpolation scheme.
 348 SIMP makes use of gradients to make incremental
 349 changes to the shape followed by the application
 350 of morphological filters³⁹. In this paper, the im-
 351 plementation is adapted from the efficient 88-line
 352 code for compliance minimisation by Andreassen
 353 et al.³⁸ replacing compliance and its gradients
 354 with absorption and its gradients, and making
 355 the material choices as air and porous material
 356 instead of solid and void. SIMP takes the desired
 357 volume fraction (\bar{V}_f) as one of its algorithmic
 358 parameters. Two variants are considered namely,
 359 SIMPrestart and SIMPsweep.

360 1. SIMPrestart

361 In SIMPrestart, multiple trials of SIMP are
 362 run with each trial using a different \bar{V}_f . For each
 363 of these trials, SIMP was initialised from a random
 364 solution normalised to have an overall initial vol-
 365 ume fraction close to the chosen \bar{V}_f . Once conver-
 366 gence is achieved, SIMP is restarted with a new \bar{V}_f
 367 and a newly generated initial solution. Depending
 368 on \bar{V}_f and the initial solution, the algorithm con-
 369 verges to a variety of shapes as Figure 3(a) shows
 370 for problem instance 6. Each trial converged af-
 371 ter about 100 iterations. The process is continued
 372 until the budget of 1365 is used up.

373 To populate the Pareto front, equispaced val-
 374 ues of \bar{V}_f were used in each trial. The solution
 375 progress in the objective space from SIMPrestart
 376 for all trials are shown in figure 3(b) for problem
 377 instance 6.

378 2. SIMPsweep

379 SIMPsweep starts from an empty or air-filled
 380 solution with an initial volume fraction limit $\bar{V}_f =$

381 0, and applies SIMP move updates while updating
 382 \bar{V}_f in every iteration reaching $\bar{V}_f = 1$ as the fit-
 383 ness evaluation budget is reached. The solutions
 384 produced for problem instance 6 are plotted in the
 385 objective space in Figure 4, along with some of the
 386 shapes. It can be observed that as the volume frac-
 387 tion increases, the general trend is that absorption
 388 also increases. Notably for this melamine problem
 389 instance, some of the optimal shapes closely resem-
 390 ble flat layers. Whereas this is not always the case
 391 across problem instances.

392 The solutions from SIMP algorithms did not
 393 always result in 0 or 1 shapes, and the shapes were
 394 rounded i.e., values less than 0.5 are set to 0 and
 395 more than 0.5 are set to 1, and the absorptions
 396 were recomputed. This involved additional fitness
 397 evaluations beyond the budget. Nevertheless, the
 398 resulting changes in absorption due to rounding
 399 were insignificant in most cases.

400 A comparison of Pareto fronts of SIMPsweep
 401 and SIMPrestart is shown in Figure 6 for problem
 402 instance 6. It may be observed that for some vol-
 403 ume fraction values ($V_f \approx 0.1$) SIMPsweep found
 404 better solutions while in others ($V_f \approx 0.6$) SIM-
 405 Pstart did. In this problem instance, SIMPsweep
 406 seems to cover a larger hypervolume. However,
 407 upon observing the hypervolumes for all problem
 408 instances in Table V, there seems to be no clear
 409 winner between SIMPrestart and SIMPsweep since
 410 the former covered more hypervolumes in three
 411 problem instances while the latter covered more
 412 in the other four.

413 Among the two, for lower fitness evaluation
 414 budgets, SIMPsweep is recommended since unlike
 415 in SIMPrestart, less computational time will be
 416 spent on initially reaching good solutions as also
 417 suggested by Suresh²³.

418 B. Constructive heuristic using gradient (CHg)

419 Constructive heuristics are methods which in-
 420 crementally build solutions from scratch. In a
 421 previous study, a material-addition constructive
 422 heuristic (CH1) performed among the best ap-
 423 proaches in topology optimisation for maximising
 424 sound absorption⁹. In CH1, the procedure was
 425 to incrementally add porous materials to locations
 426 where the increase in absorption would be the high-
 427 est. However, finding the change in absorption at
 428 every finite element is computationally expensive
 429 and in this approach (CHg), they are replaced by
 430 gradients which are relatively cheap (Equation 3).
 431 CHg starts from an empty or air-filled design do-
 432 main, and fills porous material incrementally in
 433 finite elements where the gradient of sound ab-
 434 sorption $\frac{\partial \alpha}{\partial \chi_i}$ is highest. At each step m number
 435 of elements are chosen to fill with porous material
 436 after each gradient evaluation, and the total num-
 437 ber of fitness evaluations necessary would be n_e/m
 438 where n_e is the total number of elements. m is cho-
 439 sen such that n_e/m does not exceed the budget.

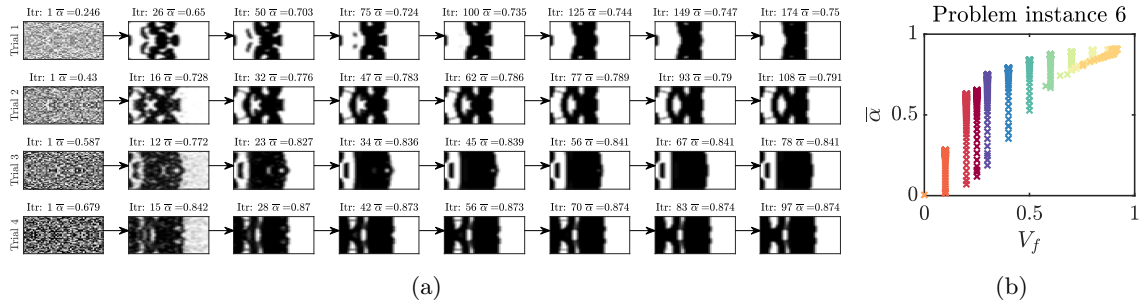


Figure 3. SIMPrestart:(a) Best shapes from the first 4 trials on problem instance 6 with volume fraction limits 0.3, 0.4, 0.5 and 0.6 respectively. In these shape images and others, the rigid backing is on the right and the acoustic forcing is on the left. (b) Progress in objective space for various trials. Each colour corresponds to a different trial with different \bar{V}_f .

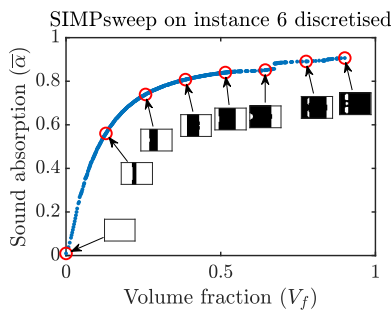


Figure 4. (color online) SIMPsweep: Pareto front for problem instance 6, which uses melamine, results in shapes that resemble flat layers.

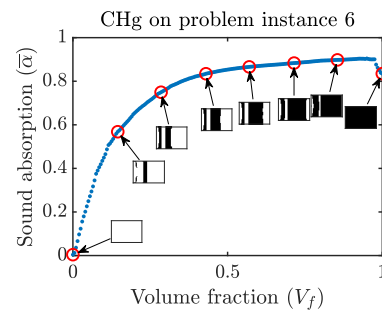


Figure 5. (color online) Solution progress for constructive heuristic using gradients (CHg) applied on problem instance 6

440 Note that in the seven problem instances consid-
 441 ered, the number of elements are respectively 100,
 442 150, 1000, 100, 100,1000, and 50. Since the bud-
 443 get considered is 1365, all problem instances can
 444 be completed in n_e fitness evaluations with $m = 1$.
 445 Hence, CHg will effectively utilise less fitness eval-
 446 uations than the budget in the cases considered.
 447 Note that CHg always will search solutions in the
 448 discrete space since an element is either filled or
 449 not filled. In this way, it is different from SIMP-
 450 sweep.

451 The progress of solutions found by CHg applied
 452 on problem 6 instance is shown in Figure 5 in
 453 the objective space along with a few shapes. Here,
 454 the shapes have two flat layers as opposed to one
 455 as found in SIMPsweep.

456 C. Comparing gradient-based approaches

457 Figure 6 compares the Pareto fronts produced
 458 by SIMPrestart, SIMPsweep and CHg algorithms
 459 for problem instance 6 as an example. Note
 460 that while SIMPrestart tends to leave gaps in the
 461 Pareto front, SIMPsweep and CHg finds more so-
 462 lutions and span the front well. There are specific
 463 regions where one algorithm performs better than

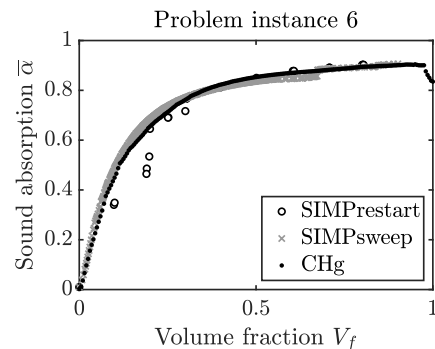


Figure 6. Comparison of gradient methods SIMPrestart, SIMPsweep and CHg for problem instance 6.

464 the other two, but overall, these three approaches
 465 can be considered to be similar in terms of perfor-
 466 mance.

467 The hypervolumes covered by solutions from
 468 the gradient approaches are shown in Table IV.
 469 Among the three methods, SIMPrestart covered
 470 the most hypervolume in one problem instance,
 471 SIMPsweep in two problem instances and CHg in
 472 the other four, as emphasised by the bold font.

Table IV. Hypervolume comparison of gradient based approaches SIMPstart, SIMPsweep and CHg

Instance	SIMPstart	SIMPsweep	CHg
1	0.7065	0.6835	0.6724
2	0.4014	0.4047	0.4066
3	0.7317	0.6063	0.7412
4	0.1160	0.1188	0.1087
5	0.5208	0.5292	0.5323
6	0.7202	0.7607	0.7512
7	0.8727	0.8567	0.8733

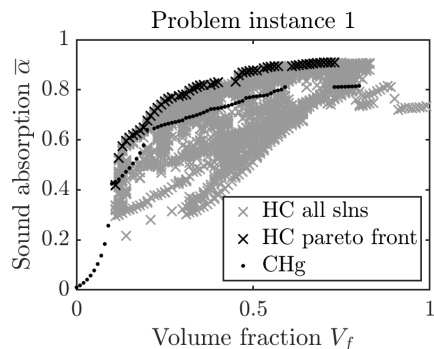


Figure 7. Solutions traversed by hill climbing (HC) with combined Pareto front from 15 trials compared against CHg Pareto front. HC finds improvements over CHg.

473 However, the values are not significantly different
474 among the three approaches.

475 An important aspect to note is the possibility
476 to speed up SIMPsweep and CHg if required. For
477 instance, if only $1/10^{th}$ of the fitness evaluation
478 budget is allowed, in SIMPsweep, the volume frac-
479 tion constraint \bar{V}_f would be adapted 10 times more
480 quickly to reach 1 as the budget is used up. Sim-
481 ilarly for CHg, one can simply increase m which
482 is to add more elements with porous material in
483 each iteration. Though this risks potentially miss-
484 ing several trade-off solutions, the quality of the so-
485 lutions would not be significantly affected. This is
486 because, every next solution found by SIMPsweep
487 or CHg is an incremental perturbation from an al-
488 ready good solution. Although, for SIMPstart,
489 speed-up can be achieved by tuning the move limit
490 parameter m^{38} , there are some caveats to doing
491 this such as the occurrence of numerical oscilla-
492 tions.

493 IV. NON-GRADIENT APPROACHES

494 A. Hill climbing

495 Hill climbing is a heuristic for single objective
496 optimisation. Typically, a single initial solution is

497 picked and iteratively modified, and the modified
498 solution is accepted as the current solution if it is
499 improving.

500 In this implementation, to allow choosing ini-
501 tial solutions spread out in volume fraction, a de-
502 sired volume fraction is first picked randomly be-
503 tween 0 and 1, and this value is used as the prob-
504 ability to fill porous material in each element.

From the initial solution, elements are bit-
flipped row-by-row, and the change is accepted if
the scalarised objective function decreases. This
is similar to HC in Ramamoorthy et al.⁹ but with
a weighted-sum scalarisation, in which the two ob-
jectives are combined into one as given in Equation
4.

$$\min_{\mathbf{x}} C = -w\bar{\alpha} + (1-w)V_f \quad (4)$$

505 The weight w corresponds to the importance of
506 maximising absorption as opposed to minimising
507 volume fraction and can take values between 0 and
508 1. A weight of 1 implies maximising only absorp-
509 tion irrespective of volume fraction, and likewise, a
510 weight of 0 corresponds to only minimising volume
511 fraction. An illustration of the effect of choosing
512 w on the scalarised objective is shown in Figure 8.
513 Note that w governs the slope of the isolines of the
514 scalarised objective. This will be relevant later.

515 For each trial run of HC, a fixed weight is cho-
516 sen. Then, hill climbing on the combined objective
517 is done until the fitness evaluation budget is used
518 up. 15 such trials are run with different weights.
519 Figure 7 shows all solutions from 15 trials of HC
520 for problem instance 1 compared with CHg solu-
521 tions. The trails of points in the figure correspond
522 to individual trials improving solutions in a specific
523 direction depending on the chosen weight. The
524 combined results from HC are better than those
525 of CHg in some regions in both $\bar{\alpha}$ and V_f , indicat-
526 ing that the gradient methods do often converge to
527 local-optimal solutions, and potential for improve-
528 ments exist.

529 An issue with HC is that only a specific re-
530 gion in the Pareto front will be explored in a given
531 trial. The trial-averaged hypervolumes are signifi-
532 cantly lower than the combined hypervolume over
533 15 trials as may be observed by comparing the HC
534 columns in Tables V and VI. This is because us-
535 ing a set scalarisation weight for a trial guides the
536 search towards a specific region in the Pareto front.

537 B. Non-dominated sorting genetic algorithms (NSGA- 538 II)

539 NSGA-II is a popular multi-objective optimi-
540 sation strategy introduced by Deb et al²⁸. It
541 has been effectively used in solving multi-criteria
542 decision-making problems across a plethora of
543 fields. In this implementation, a single-point cross
544 over with an individual cross-over probability of 0.9
545 is applied with a bit-wise mutation rate of $(1/n_e)$

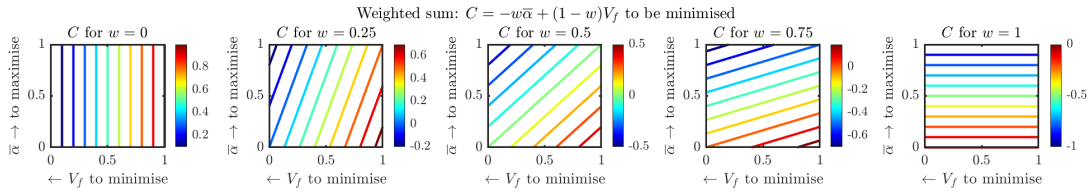


Figure 8. (color online) The effect of weights in weighted-sum scalarisation on the slope of the isolines of combined objective value.

546 where n_e is the chromosome length and a popula-
 547 tion size of 32. These parameters were found using
 548 parameter-tuning studies on genetic algorithms⁹.
 549 Figure 9 shows the progress of solutions in the
 550 objective function space for one trial of NSGA-II
 551 for problem instance 1. In the figure, each point
 552 refers to a particular shape and the colour corre-
 553 sponds to the generation in which it was found. We
 554 can observe that as the generations progress (from
 555 blue towards red), the solutions tend towards more
 556 sound absorption and less volume fraction.

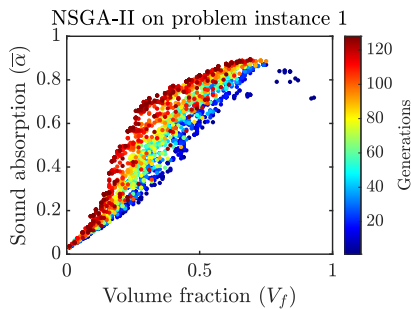


Figure 9. (color online) NSGA-II progress of solutions in the objective function space for problem instance 1 trial 1.

557 C. Random Search (RAND)

558 For benchmarking the performance of HC and
 559 NSGA-II, a random search algorithm referred here
 560 as RAND is applied on all seven problem instances.
 561 Random solutions spread across volume fraction
 562 are obtained by choosing a random number for de-
 563 sired volume fraction, and using this value as prob-
 564 ability to fill porous material in each element. 4096
 565 such solutions are generated and fitnesses are eval-
 566 uated in each trial, and 15 such trials were run. Us-
 567 ing non-dominated sorting on each trial separately
 568 and across all 15 trials, the trial-averaged and 15-
 569 trial-combined hypervolumes were found and pop-
 570 ulated in tables V and VI.

571 D. Comparison of non-gradient algorithms

572 1. Performance per trial

573 Comparing the median-trial hypervolumes
 574 from HC and NSGAII in Table V, it is clear that
 575 NSGA-II is consistently better across all problem
 576 instances. This is because based on the choice
 577 of scalarisation weight, in a given trial, HC only
 578 explores a specific region in the Pareto front.
 579 Whereas, NSGA-II spans the objective space effec-
 580 tively due to the crowding distance-based selection
 581 mechanism. NSGA-II also outperforms RAND in
 582 all problem instances, but interestingly, HC on a
 583 per-trial basis, does not outperform even RAND.
 584 Moreover, RAND outperforms HC across all prob-
 585 lem instances. This is because HC in a single trial
 586 is essentially a single-objective algorithm that does
 587 not incentivise spanning the hypervolume.

588 2. Performance across 15 trials combined

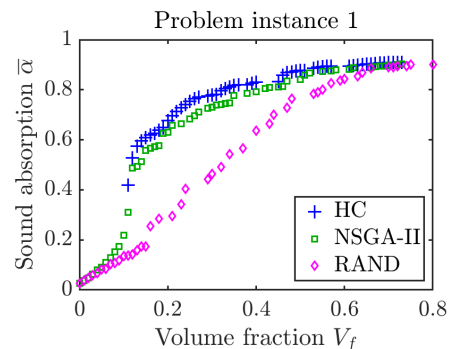


Figure 10. (color online) Combined Pareto fronts from 15 trials of HC, NSGA-II and RAND on problem instance 1.

589 Combining 15 trials of HC run with different
 590 weights results in a better hypervolume than com-
 591 bined results of 15 trials of NSGA-II consistently
 592 across all problem instances as can be observed in
 593 Table VI (see columns HC vs NSGA-II). As an ex-
 594 ample, for problem instance 1, by comparing the
 595 Pareto fronts in Figure 10, it is clear that HC so-
 596 lutions often have better absorption for the same
 597 volume fraction than NSGA-II. Both NSGA-II and

598 HC cover a larger hypervolume than RAND by a
599 large margin.

600 V. HYBRID APPROACHES

601 From the studies on gradient and non-gradient
602 algorithms, it was evident that gradient methods
603 can quickly approximate the Pareto front, whereas
604 non-gradient methods can provide improvements
605 in specific regions of the Pareto front.

606 In order to obtain the benefits of both, two hy-
607 brid approaches combining a gradient-based algo-
608 rithm for initiation and a non-gradient algorithm
609 for improvement is presented and compared. The
610 first hybrid approach is a combination of CHg and
611 HC denoted as HA1, and the second hybrid ap-
612 proach is a combination of CHg and NSGA-II de-
613 noted as HA2. We picked CHg as the initiator
614 mainly because, it guarantees discrete solutions
615 and allows the possibility to speed up (see III C).

616 A. Hybrid approach 1: CHg+HC

617 Hybrid approach 1 (HA1) combines the use of
618 CHg for 25% of the budget and HC for the remain-
619 ing 75% of the budget. These numbers are arbi-
620 trarily chosen with some basis on experience. Since
621 CHg is gradient-based, and gradient-included eval-
622 uations are thrice as expensive as non-gradient fit-
623 ness evaluations (Equation 3), the rationing is such
624 that CHg uses $25\% \times (\frac{4096}{3})$ fitness evaluations and
625 HC uses $75\% \times (\frac{4096}{1})$.

626 Figure 11 illustrates the procedure involved in
627 HA1. Firstly, CHg is run to obtain a trade-off so-
628 lution set. Then, 15 solutions are selected from
629 the CHg trade-off set equispaced in volume frac-
630 tion to use as initial solutions for each of the 15
631 HC trials. For each HC trial, a different scalari-
632 sation weight w is used such that the isolines of
633 the combined objective C has a slope tangential to
634 CHg Pareto front at the initial solution. The slope
635 of the Pareto front at the initial solution is ob-
636 tained using a simple central difference of adjacent
637 points. This ‘Pareto-slope-based scalarisation’ ef-
638 fectively guides HC to find improvements to the
639 Pareto front. HC is run until the remaining bud-
640 get is used up. As seen in Figure 11, in each trial,
641 only a specific region is explored. The hypervol-
642 umes covered after each trial and after combining
643 all 15 trials are computed.

644 The per-trial median hypervolumes and 15-
645 trials-combined hypervolumes obtained by HA1
646 are provided in Tables V and VI for all problem
647 instances.

648 B. Hybrid approach 2: CHg+NSGA-II

649 Hybrid approach 2 (HA2) combines CHg and
650 NSGA-II in a similar fashion i.e., CHg uses 25% of
651 the budget, NSGA-II uses the remaining 75%. The

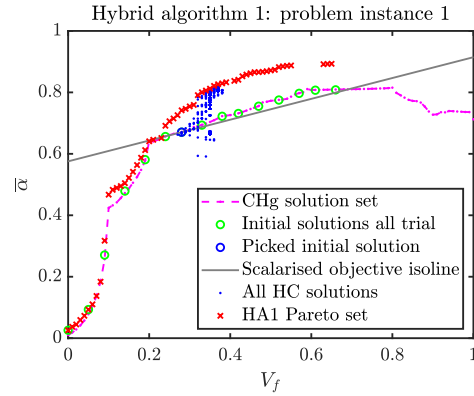


Figure 11. (color online) Hybrid approach 1 illustration of a trial for problem instance 1. Apply CHg for 25% of the budget. Pick an initial solution on the CHg Pareto set. Set scalarisation weight such that the isolines of the combined objective are tangential to the Pareto front at the selected CHg point. Apply hill climbing for the rest of the fitness evaluation budget. The final Pareto set after combining 15 trials each starting from equispaced points on the CHg Pareto set are shown using ‘x’ markers.

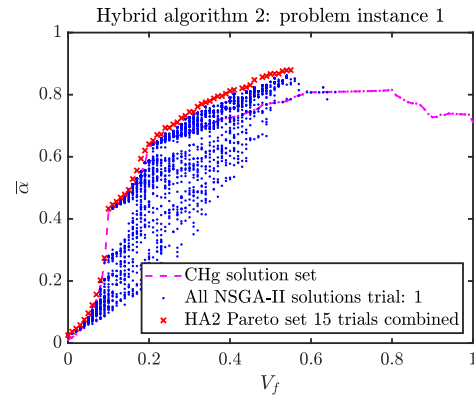


Figure 12. (color online) Hybrid approach 2: CHg run for 25% of computational budget, and then using the Pareto set as the initial population, NSGA-II is run for the remaining budget. Solutions traversed by NSGA-II in one of the 15 trials are shown in blue dots. The combined Pareto front from 15 trials is shown in red crosses.

652 rationing of fitness evaluations is similar to that in
653 HA1.

654 Originally, the final solution set from CHg was
655 meant to be used as the initial population for
656 NSGA-II in each trial. However, on some occasions
657 the CHg Pareto front contained more or less solu-
658 tions than the population size assigned for NSGA-
659 II. Hence, when there were more solutions in CHg
660 Pareto set, only 32 solutions equispaced in volume
661 fraction were considered as the initial population
662 for NSGA-II, and when there were less solutions,

663 they were duplicated using the selection process in
664 the first generation. Then NSGA-II is run for the
665 remainder of the budget.

666 Figure 12 shows the solutions searched in an
667 example trial out of the 15 trials that were run for
668 problem instance 1. The combined Pareto front
669 from 15 trials is then plotted using red crosses.
670 It may be observed that in the low volume frac-
671 tion regions, the solutions from NSGA-II never
672 seem to improve. This is because crossover and
673 mutation operations always produced worse solu-
674 tions. The hypervolumes covered by the median
675 trial and the overall hypervolume of the combined
676 non-dominated solutions across 15 trials of HA2
677 are provided in Tables V and VI.

678 C. Overall comparison

679 1. Trial-averaged performance for 4096 budget

680 For a computational budget of 4096 gradient-
681 free fitness evaluations, Table V shows the result-
682 ing hypervolumes covered by all algorithms used
683 in this study. It should be noted that CHg did
684 not need to use the entire budget. Since in each
685 iteration, CHg has to fill at least one element, the
686 entire design domain can be filled with only {100,
687 150, 1000, 100, 100, 1000, 50} fitness evaluations
688 respectively for problem instances 1 through 7.

689 Keeping this in mind, the table shows that
690 HA2, a combination of CHg and NSGA-II, cov-
691 ers the most hypervolume in 4 out of 7 prob-
692 lem instances on average per trial. Note that
693 HA2 also performs better than stand-alone NSGA-
694 II for the same budget. While it is evident
695 that gradient-based initialisation boosts the per-
696 formance of NSGA-II, it is interesting to note
697 that HA2 can perform better than SIMPstart or
698 SIMPsweep which are normally used in practise.
699 Thus, if one has a fixed computational budget, to
700 cover the most hypervolume, a reliable strategy is
701 to use a combination of CHg followed by NSGA-II.

702 Also, it is worth noting that SIMPsweep per-
703 forms the best in two problem instances and CHg
704 performs best in one problem instance. Notably,
705 SIMPsweep and CHg are also scalable for lower
706 budgets. These three algorithms may be recom-
707 mended for applications such as software imple-
708 mentations in the initial stages of design that need
709 to quickly come up with trade-off acoustic solu-
710 tions within a set computational budget.

711 2. Combined performance of 15 trials each with 712 4096 budget

713 It is also of interest to identify effective strate-
714 gies that find solutions with best attainable qual-
715 ity with relaxed computational time budgets, such
716 as for manufacturing best acoustic designs. Ta-
717 ble VI shows the resulting hypervolumes covered
718 by a combination of 15 trials which is equivalent
719 to 15×4096 gradient-free function evaluations. For

720 this comparison, we do not include the gradient
721 methods as they did not use the same budget.

722 In this study, HC shows a significant improve-
723 ment as it is able to combine the good solutions
724 from various regions of the Pareto front. For the
725 same reason HA1 (CHg+HC) also performs excep-
726 tionally well, producing the best hypervolumes in
727 6 out of 7 problem instances. This shows that the
728 proposed Pareto-slope-based weighted-sum scalar-
729 isation technique with a simple greedy hill climb-
730 ing algorithm can be used as an effective local
731 improvement strategy. A take-away is that be-
732 fore manufacturing an optimal shape using any
733 multi-objective topology optimisation approach, it
734 is worth ensuring that there exists no other domi-
735 nating solution that HC can find.

736 Between NSGA-II and its hybrid counterpart
737 HA2, the latter seems to cover more hypervolumes
738 across all problem instances. This is again an ex-
739 ample of a hybrid approach performing better than
740 its parent approach. HA2 also performed the best
741 in one of the seven problem instances, and comes
742 close to the performance of HA1. This show that
743 there is benefit to using hybrid strategies involving
744 gradient initialisers with non-gradient improvers.

745 3. Pareto front comparison for all algorithms 746 combined across 15 trials

747 The problem of topology optimisation has no
748 exact algorithms that run in practical times to con-
749 firm the true Pareto-optimal solutions. Neverthe-
750 less, it is of interest to see which algorithms con-
751 tribute to finding the best known solutions in the
752 Pareto diagram.

753 Hence, we compare the Pareto fronts obtained
754 from all algorithms in one place. As an example,
755 this is shown for problem instance 1 in Figure 13.
756 The gradient algorithms are marked in blue, non-
757 gradient in red and hybrid in green.

758 It should be noted that the Pareto fronts for
759 gradient algorithms are obtained from only one
760 trial, while results for other algorithms are from a
761 combination of 15 trials. Hence, one cannot draw
762 a direct comparison across gradient strategies and
763 others.

764 Among the three gradient algorithms, it may
765 be observed that CHg finds better absorbing solu-
766 tions in lower volume fractions up to 0.3, and
767 the SIMP algorithms found better solutions after
768 $V_f = 0.3$.

769 Among non-gradient algorithms, it is clear
770 that all approaches perform better than random
771 search, but there is no single clear winner between
772 HC and NSGA-II.

773 Hybrid algorithms work best to cover the most
774 hypervolume, but interestingly, there are some re-
775 gions where HC produces better non-dominated
776 solutions (see between $V_f=0.1$ and 0.3). This
777 shows that one cannot ignore HC just because the

Table V. Median hypervolumes obtained while running one trial with a budget equivalent to 4096 gradient-free fitness evaluations. HA2 seems to perform best when considering the trial-averaged performance for 4096 fitness evaluations.

Fitness evaluations	Gradient-based			Gradient-free			Hybrid	
	1365	1365	$\min(n_e/m, 1365)$	4096	4096	4096	4096	4096
Instance/ Alg	SIMPstart	SIMP sweep	CHg	HC	NSGAI	RAND	HA1	HA2
1	0.7065	0.6835	0.6724	0.5622	0.6824	0.5915	0.7013	0.7170
2	0.4014	0.4047	0.4066	0.2684	0.3427	0.3212	0.4066	0.4068
3	0.7317	0.6063	0.7412	0.5908	0.6336	0.6061	0.7343	0.7184
4	0.1160	0.1188	0.1087	0.0893	0.1148	0.1085	0.1122	0.1174
5	0.5208	0.5292	0.5323	0.3798	0.4847	0.4561	0.5324	0.5327
6	0.7202	0.7607	0.7512	0.5430	0.6159	0.6211	0.7603	0.7601
7	0.8727	0.8567	0.8733	0.7133	0.8531	0.7677	0.8733	0.8758

Table VI. Hypervolume combined over 15 trials are compared in this table. These hypervolumes are also contrasted with those of single trials of gradient algorithms. HA1 seems to perform consistently better when considering a combination of 15 trials of 4096 fitness evaluations.

Instance	Gradient-free			Hybrid	
	HC	NSGAI	RAND	HA1	HA2
Budget	15*4096	15*4096	15*4096	15*4096	15*4096
1	0.7436	0.7302	0.6221	0.7438	0.7307
2	0.4029	0.3613	0.3329	0.4081	0.4074
3	0.7772	0.6878	0.6219	0.8104	0.7295
4	0.1144	0.1169	0.1107	0.1195	0.1190
5	0.5212	0.5034	0.4708	0.5343	0.5337
6	0.7509	0.6310	0.6269	0.7646	0.7606
7	0.8407	0.8725	0.8021	0.8755	0.8759

hypervolume spanned is poor. The potential of HC for local exploration needs to be recognised.

VI. CONCLUSION

In this article, several multi-objective strategies were compared to identify effective approaches for quickly obtaining lightweight and high-absorbing acoustic shape designs within a given amount of computational effort. Three gradient strategies—SIMPstart, SIMP sweep and CHg, two gradient-free strategies—HC and NSGA-II, and two hybrid strategies—HA1 (CHg+HC) and HA2 (CHg+NSGA-II), were studied. The findings are highlighted as follows.

1. Gradient algorithms often get stuck at local-optimal shapes indicated by the fact that non-gradient approaches have been able to find better solutions in terms of both absorption and volume fraction objectives.

2. Reusing solutions from SIMP with an adaptive volume fraction constraint (SIMP sweep) is better at spanning the Pareto front than restarting SIMP at various volume fraction constraints (SIMPstart).

3. A simple new gradient-based constructive heuristic (CHg) is introduced that guarantees discrete solutions while also being scalable and as performant as SIMP algorithms.

4. Hybrid approaches using gradient algorithms as initialisers and non-gradient algorithms as exploiters seem to be more effective than any parent gradient or non-gradient algorithm for the same computational budget.

5. Hill climbing with a Pareto-slope-based weighted-sum scalarisation proves to be an effective local search technique to improve solutions near the Pareto front.

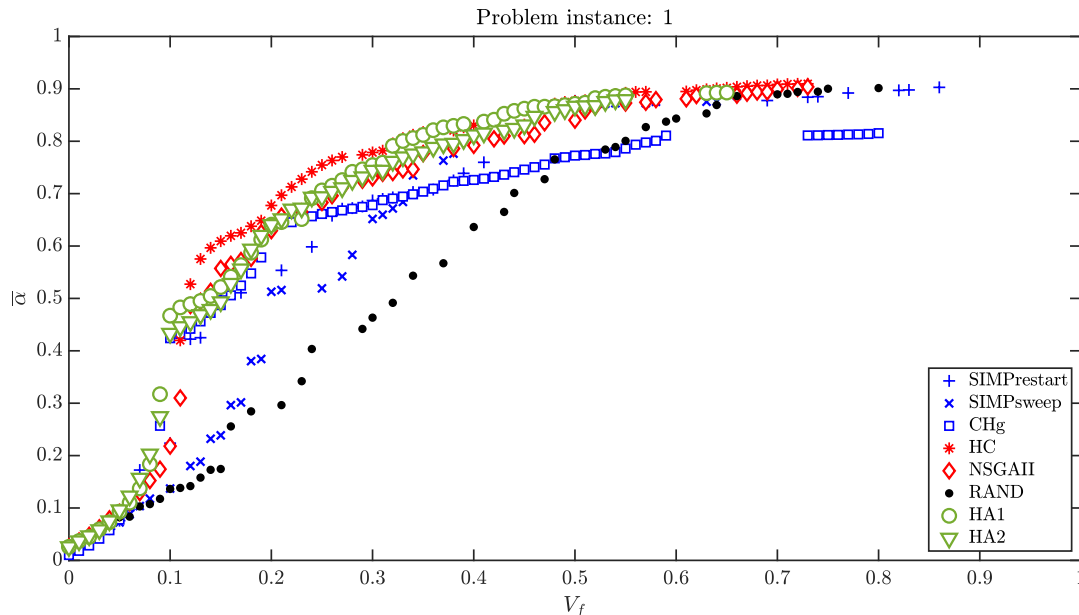


Figure 13. (color online) Comparison of non-dominated solutions from all algorithms for problem instance 1. Colours blue, red and green correspond to gradient, non-gradient and hybrid algorithms respectively. Gradient algorithm results are from one trial, whereas non-gradient and hybrid algorithm results are from a combination of 15 trials. Hence they must not be compared.

814 If the goal is to quickly find a set of trade-off
 815 shapes, such as to use in software applications,
 816 then any gradient approach or a hybrid approach
 817 with CHg and NSGA-II would be more suitable. If
 818 the goal is to obtain the optimised shape designs of
 819 the best attainable quality for manufacture, then a
 820 hybrid approach with CHg and hill climbing with a
 821 Pareto-slope-based scalarisation seems to be more
 822 suitable. If the interest is to find the best attain-
 823 able trade-off solutions to a problem, then no algo-
 824 rithm is a clear winner. Algorithms such as HC oc-
 825 casionally find better solutions in specific regions
 826 than their hybrid counterpart and cannot be ig-
 827 nored.

828 ACKNOWLEDGEMENT

829 This result is part of a project that received
 830 funding from the European Research Coun-
 831 cil (ERC) under the European Union’s Hori-
 832 zon 2020 research and innovation programme
 833 *No2Noise* (no2noise.eu) with the grant agreement
 834 no. 765472.

835 REFERENCES

836 ¹Tristan Cambonie, Fulbert Mbailassem, and Emmanuel
 837 Gourdon. Bending a quarter wavelength resonator: Cur-
 838 vature effects on sound absorption properties. *Applied*
 839 *Acoustics*, 131:87–102, 2018.

840 ²Joong Seok Lee, Yoon Young Kim, Jung Soo Kim, and
 841 Yeon June Kang. Two-dimensional poroelastic acoustical
 842 foam shape design for absorption coefficient maximization
 843 by topology optimization method. *The Journal of the*

844 *Acoustical Society of America*, 123(4):2094–2106, 2008.

845 ³Won Uk Yoon, Jun Hyeong Park, Joong Seok Lee, and
 846 Yoon Young Kim. Topology optimization design for total
 847 sound absorption in porous media. *Computer Methods in*
 848 *Applied Mechanics and Engineering*, 360:112723, 2020.

849 ⁴Ole Sigmund and Kurt Maute. Topology optimization ap-
 850 proaches. *Structural and Multidisciplinary Optimization*,
 851 48(6):1031–1055, 2013.

852 ⁵Martin P Bendsøe and N Kikuchi. Generating optimal
 853 topologies in structural design using a homogenization
 854 method. *Computer methods in applied mechanics and*
 855 *engineering*, 71(2):197–224, 1988.

856 ⁶Martin P Bendsøe. Optimal shape design as a material
 857 distribution problem. *Structural optimization*, 1(4):193–
 858 202, 1989.

859 ⁷Eddie Wadbro and Martin Berggren. Topology optimiza-
 860 tion of an acoustic horn. *Computer methods in applied*
 861 *mechanics and engineering*, 196(1-3):420–436, 2006.

862 ⁸Maria B Dühring, Jakob S Jensen, and Ole Sigmund.
 863 Acoustic design by topology optimization. *Journal of*
 864 *sound and vibration*, 317(3-5):557–575, 2008.

865 ⁹Vivek T. Ramamoorthy, Ender Özcan, Andrew J. Parkes,
 866 Abhilash Sreekumar, Luc Jaouen, and François-Xavier
 867 Bécot. Comparison of gradient-based and gradient-free
 868 heuristics and metaheuristics for topology optimisation
 869 in acoustic porous materials. *The Journal of the Acous-
 870 tical Society of America*, 150(4):3164–3176, 2021.

871 ¹⁰Jin Woo Lee and Yoon Young Kim. Topology optimiza-
 872 tion of muffler internal partitions for improving acoustical
 873 attenuation performance. *International journal for*
 874 *numerical methods in engineering*, 80(4):455–477, 2009.

875 ¹¹Gil Ho Yoon. Acoustic topology optimization of fibrous
 876 material with Delany–Bazley empirical material formula-
 877 tion. *Journal of Sound and Vibration*, 332(5):1172–1187,
 878 2013.

879 ¹²Joong Seok Lee, Peter Göransson, and Yoon Young Kim.
 880 Topology optimization for three-phase materials distribu-
 881 tion in a dissipative expansion chamber by unified multi-

- 882 phase modeling approach. *Computer Methods in Applied*
883 *Mechanics and Engineering*, 287:191–211, 2015.
- 884 ¹³Esubalewe Lakie Yedeg, Eddie Wadbro, and Martin
885 Berggren. Interior layout topology optimization of a reac-
886 tive muffler. *Structural and Multidisciplinary Optimiza-*
887 *tion*, 53(4):645–656, 2016.
- 888 ¹⁴Junghwan Kook, Kunmo Koo, Jaeyub Hyun, Jakob S
889 Jensen, and Semyung Wang. Acoustical topology opti-
890 mization for Zwicker’s loudness model—application to
891 noise barriers. *Computer methods in applied mechanics*
892 *and engineering*, 237:130–151, 2012.
- 893 ¹⁵Ki Hyun Kim and Gil Ho Yoon. Optimal rigid and
894 porous material distributions for noise barrier by acoustic
895 topology optimization. *Journal of Sound and Vibration*,
896 339:123–142, 2015.
- 897 ¹⁶Leilei Chen, Cheng Liu, Wenchang Zhao, and Linchao
898 Liu. An isogeometric approach of two dimensional acous-
899 tic design sensitivity analysis and topology optimization
900 analysis for absorbing material distribution. *Computer*
901 *Methods in Applied Mechanics and Engineering*, 336:507–
902 532, 2018.
- 903 ¹⁷Zi-xiang Xu, Hao Gao, Yu-jiang Ding, Jing Yang, Bin
904 Liang, and Jian-chun Cheng. Topology-optimized omni-
905 directional broadband acoustic ventilation barrier. *Phys-*
906 *ical Review Applied*, 14(5):054016, 2020.
- 907 ¹⁸Yanming Xu, Wenchang Zhao, Leilei Chen, and Haibo
908 Chen. Distribution optimization for acoustic design of
909 porous layer by the boundary element method. *Acoustics*
910 *Australia*, pages 107–119, 2020.
- 911 ¹⁹Hans A Eschenauer and Niels Olhoff. Topology optimiza-
912 tion of continuum structures: a review. *Appl. Mech. Rev.*,
913 54(4):331–390, 2001.
- 914 ²⁰George IN Rozvany and Tomasz Lewiński. *Topology*
915 *optimization in structural and continuum mechanics*.
916 Springer, 2014.
- 917 ²¹Jikai Liu, Andrew T Gaynor, Shikui Chen, Zhan Kang,
918 Krishnan Suresh, Akihiro Takezawa, Lei Li, Junji Kato,
919 Jinyuan Tang, Charlie CL Wang, et al. Current and fu-
920 ture trends in topology optimization for additive manu-
921 facturing. *Structural and multidisciplinary optimization*,
922 57(6):2457–2483, 2018.
- 923 ²²Ole Sigmund. A 99 line topology optimization code writ-
924 ten in Matlab. *Structural and multidisciplinary optimiza-*
925 *tion*, 21(2):120–127, 2001.
- 926 ²³Krishnan Suresh. A 199-line Matlab code for pareto-
927 optimal tracing in topology optimization. *Structural and*
928 *Multidisciplinary Optimization*, 42(5):665–679, 2010.
- 929 ²⁴Amir M Mirzendehtdel and Krishnan Suresh. A pareto-
930 optimal approach to multimaterial topology optimization.
931 *Journal of Mechanical Design*, 137(10), 2015.
- 932 ²⁵Yi M Xie and Grant P Steven. A simple evolutionary pro-
933 cedure for structural optimization. *Computers & struc-*
934 *tures*, 49(5):885–896, 1993.
- 935 ²⁶YM Xie and GP Steven. Evolutionary structural opti-
936 mization for dynamic problems. *Computers & Structures*,
937 58(6):1067–1073, 1996.
- 938 ²⁷Refail Kasimbeyli, Zehra Kamisli Ozturk, Nergiz Kasim-
939 beyli, Gulcin Dinc Yalcin, and Banu Icmen Erdem. Com-
940 parison of some scalarization methods in multiobjective
941 optimization. *Bulletin of the Malaysian Mathematical*
942 *Sciences Society*, 42(5):1875–1905, 2019.
- 943 ²⁸Kalyanmoy Deb, Samir Agrawal, Amrit Pratap, and
944 Tanaka Meyarivan. A fast elitist non-dominated sort-
945 ing genetic algorithm for multi-objective optimization:
946 NSGA-II. In *International conference on parallel prob-*
947 *lem solving from nature*, pages 849–858. Springer, 2000.
- 948 ²⁹Shanu Verma, Millie Pant, and Vaclav Snel. A compre-
949 hensive review on nsga-ii for multi-objective combinato-
950 rial optimization problems. *Ieee Access*, 9:57757–57791,
951 2021.
- 952 ³⁰Weidong Liu, Hua Zhu, Yiping Wang, Shengqiang Zhou,
953 Yalei Bai, and Chunsheng Zhao. Topology optimization
954 of support structure of telescope skin based on bit-matrix
955 representation nsga-ii. *Chinese Journal of Aeronautics*,
956 26(6):1422–1429, 2013.
- 957 ³¹Xu Guo, Weisheng Zhang, and Wenliang Zhong. Do-
958 ing topology optimization explicitly and geometrically—a
959 new moving morphable components based framework.
960 *Journal of Applied Mechanics*, 81(8), 2014.
- 961 ³²Grégoire Allaire, François Jouve, and Anca-Maria
962 Toader. A level-set method for shape optimization.
963 *Comptes Rendus Mathématique*, 334(12):1125–
964 1130, 2002.
- 965 ³³Michael Yu Wang, Xiaoming Wang, and Dongming Guo.
966 A level set method for structural topology optimization.
967 *Computer methods in applied mechanics and engineering*,
968 192(1-2):227–246, 2003.
- 969 ³⁴Noureddine Atalla, Raymond Panneton, and Patricia De-
970 bergue. A mixed displacement-pressure formulation for
971 poroelastic materials. *The Journal of the Acoustical So-*
972 *cietly of America*, 104(3):1444–1452, 1998.
- 973 ³⁵David Linton Johnson, Joel Koplik, and Roger Dashen.
974 Theory of dynamic permeability and tortuosity in fluid-
975 saturated porous media. *Journal of fluid mechanics*,
976 176:379–402, 1987.
- 977 ³⁶Yvan Champoux and Jean-F Allard. Dynamic tortuosity
978 and bulk modulus in air-saturated porous media. *Journal*
979 *of applied physics*, 70(4):1975–1979, 1991.
- 980 ³⁷Denis Lafarge, Pavel Lemariner, Jean F Allard, and
981 Viggo Tarnow. Dynamic compressibility of air in porous
982 structures at audible frequencies. *The Journal of the*
983 *Acoustical Society of America*, 102(4):1995–2006, 1997.
- 984 ³⁸Erik Andreassen, Anders Clausen, Mattias Schevenels,
985 Boyan S Lazarov, and Ole Sigmund. Efficient topol-
986 ogy optimization in MATLAB using 88 lines of code.
987 *Structural and Multidisciplinary Optimization*, 43(1):1–
988 16, 2011.
- 989 ³⁹Ole Sigmund. Morphology-based black and white fil-
990 ters for topology optimization. *Structural and Multidis-*
991 *ciplinary Optimization*, 33(4-5):401–424, 2007.

